REAL-TIME FEEDBACK CONTROL OF CARBON CONTENT OF ZIRCONIUM DIOXIDE THIN FILMS USING OPTICAL EMISSION SPECTROSCOPY

Dong Ni [1], **Yiming Lou** [1], **Panagiotis D. Christofides** [1], **Sandy Lao** [2] and **Jane P. Chang** [2]

Department of Chemical Engineering
University of California, Los Angeles, CA 90095-1592

Abstract: In this work, we present a methodology for real-time carbon content feedback control of a plasma-enhanced metal organic chemical vapor deposition process using optical emission spectroscopy. Initially, an estimation model of carbon content of ZrO_2 thin films based on real-time optical emission spectroscopy data is presented. Then, a feedback control scheme, which employs the proposed estimation model and a proportional-integral controller, is developed to achieve carbon content control. Using this approach, a real-time control system is developed and implemented on an experimental electron cyclotron resonance high density plasma-enhanced chemical vapor deposition system at UCLA to demonstrate the effectiveness of real-time feedback control of carbon content. Experimental results of the deposition process under both open-loop and closed-loop operations are shown and compared. The advantages of operating the process under real-time feedback control in terms of higher productivity, reduced process variation and lower carbon content are demonstrated.

1. INTRODUCTION

The decrease of microelectronic device dimensions has motivated the replacement of silicon dioxide with oxides of higher dielectric constant (κ) as a dielectric layer in metal oxide semiconductor (MOS) devices. This is because for silicon dioxide layers thinner than about 1.6 nm, direct tunnelling currents through the oxide result in an exponential increase of leakage current. Significant leakage current increases the power dissipation and deteriorates the device performance and circuit stability for very large scale integrated (VLSI) circuits (Iwai and Momose, 1998; Lo *et al.*, 1997). In addition, since the minimum dimension of capacitors for 1-4 Gb dynamic random access memory (DRAM) generations falls into the deep submicron range, it is questionable whether acceptable charge storage can be achieved with SiO_2 within such small size regime.

The alternative is to use layers of a “new" high-κ dielectric, with the same equivalent oxide thickness or capacitance. A large number of high-κ candidate materials have been extensively studied. Among these candidate materials, ZrO_2 (as well as HfO_2) has several important properties which make it a leading candidate for an alternative dielectric. The dielectric constant of ZrO_2 is relatively high among the binary-metal oxides ($\kappa \sim 25$), and its thermal stability on Si is very good. Moreover, studies have indicated that pure ZrO_2 next to Si (with an ultra thin intervening SiO_x layer) remains stable up to 900°C (Copel *et al.*, 2000). In addition, ZrO_2 films have superior chemical resistance, good mechanical strength and a low leakage current level.

A variety of techniques can be used to prepare metal oxide thin films. Plasma-enhanced chemical vapor deposition (PECVD) is one of the most prominent means of preparing dielectric thin films, especially for memory devices applications, because of such advantages as low process temperature, high film growth rate and wide flexibility of deposition conditions. The use of metal-organic (MO) chemicals as precursors in PECVD of metal oxide thin films enables uniform film growth over large areas and complex surface ge-

[1] Process Control Group.
[2] Electronic Materials Synthesis and Plasma Processing Lab.

ometries. However, a potential problem of using MO precursors is the possibility of incorporation of impurities in the deposited thin film. One of the most important impurity species is carbon, which is abundant in the precursors. The incorporation of high concentration of carbon in the deposited film can negatively affect device performance by changing the dielectric constant and the leakage current density (Chaneliere *et al.*, 1998).

In general, carbon can be incorporated in the films either by forming carbides or oxides with the deposited metal or oxygen or by occupying intergranular positions among the grains of the main deposited compound in the form of cyclic or aliphatic species. Carbon incorporation can even occur simultaneously in multiple states depending on precursor, material to-be-deposited and operating conditions (Vahlas *et al.*, 1998; Maury *et al.*, 1996). Therefore, the development and implementation of real-time feedback control systems for carbon content control could improve the operation and use of MO precursors in the deposition of high-κ materials. Previous work on control of PECVD processes has mainly focused on control of deposition spatial uniformity (Armaou and Christofides, 1999) (see also (Armaou *et al.*, 2001) for results on control of plasma etching).

In this work, we present a methodology for real-time carbon content feedback control of a plasma-enhanced MOCVD process using optical emission spectroscopy (OES). Initially, an estimation model of carbon content of ZrO_2 thin films based on real-time OES data is presented. Then, a feedback control scheme, which employs the proposed estimation model and a proportional integral controller, is developed to achieve carbon content control. Using this approach, a real-time control system is developed and implemented on an experimental electron cyclotron resonance (ECR) high density PECVD system at UCLA to demonstrate the effectiveness of real-time feedback control of carbon content. Experimental results of the deposition process under both open-loop and closed-loop operations are shown and compared. The advantages of operating the process under real-time feedback control in terms of higher productivity, reduced process variation and lower carbon content are demonstrated.

2. ECR HIGH-DENSITY PECVD REACTOR

The schematic of the experimental ECR PECVD reactor system is shown in Figure 1. It consists of an ECR type microwave source, a reactor chamber, a pumping system, a pressure control system, a gas delivery system, an OES system and a computer-based real-time process control system.

Figure 2 shows the internal configuration of the reactor chamber. A 6-inch-diameter cylindrical stainless-steel chamber is surrounded by two circular coaxial electromagnets, which are 7 inches apart. An ASTeX ECR source is on top of the chamber. Microwave at 2.45 GHz is generated from the source and transmitted

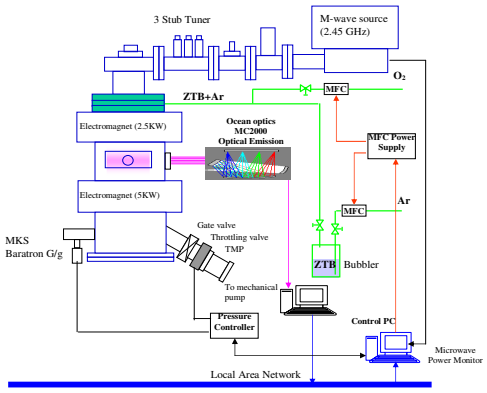

Fig. 1. Schematic diagram of the ECR plasma-enhanced CVD system used in this study.

into the chamber through a 3/8-inch thick vacuum-sealed quartz window and a high-density plasma is generated. A gas diffusion ring is located just below the top quartz window to conduct uniform distribution of the gases. A 4 inch-diameter anodized aluminum substrate holder is centered inside the chamber. The distance between the substrate holder and the top quartz window is adjustable in the range of 6.5 inches to 12 inches. The substrate holder is also connected with a 13.56 MHz radio frequency (RF) power supply tuned by a matching network; this allows controlling the ion impinging energy by applying bias voltage to the substrate.

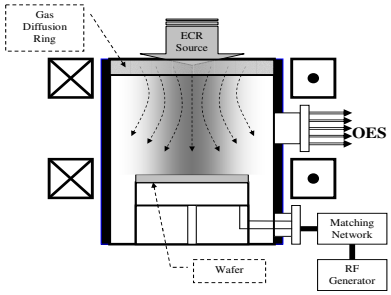

Fig. 2. Internal configuration of ECR PECVD chamber.

The chamber is pumped by a 140 l/s Alcatel 5150CP turbo-molecular pump (TMP) backed by a mechanical pump. The base pressure is measured with an HPS I-Mag cold cathode ion gauge. The chamber pressure can be controlled and varied between the base pressure and atmospheric pressure. The MKS 651C pressure controller takes the measurement of chamber pressure by an MKS 626A Baratron gauge as input and manipulates an MKS 253B throttle valve, thereby allowing to control the pressure independently from the gas flow rates.

We chose zirconium tetra-tert-butoxide $[Zr(OC_4H_9)_4]$ (ZTB) as our MO precursor because it has a sufficiently high vapor pressure (0.26 mbar at 60 ^{o}C) (Frenck *et al.*, 1991). A bubbler, which is kept at constant temperature (65 ^{o}C), is used for precursor delivery because ZTB is a liquid at room temperature (boiling point=90 ^{o}C). Ar is used as a carrier gas of the precursor vapor and the gas line is heated to 80 ^{o}C

to prevent the condensation of precursors. O_2 is used as an oxidant and mixed with Ar and ZTB at a point 8 inches away from the entrance to the reactor.

Throughout this study, the electric currents are fixed at 120 A for the 5 kW top magnet and 150 A for the 2.5 kW bottom magnet. The distance between the top quartz window and the substrate holder is kept constant at 6.5 inches and no bias is applied to the substrate.

3. OPTICAL EMISSION SPECTROSCOPY SYSTEM

Optical emission spectroscopy (OES) is the central real-time measurement tool used in this study. We use an Ocean Optics MC2000 OES system with five channels covering the wavelength range from 200 nm to 1000 nm to analyze the plasma. Each channel consists of independent optic setups including slits, gratings, a 2048-element linear silicon charged coupled diode (CCD) array and an optic fiber cable. The configurations of individual channels are shown in Table 1. The best optical resolution [full width at half maximum] for this system is 1.4 Å with a 10 μm slit width in the ultraviolet (UV) range. The integration time can be set within the range of 3 ms to 60 s. A sapphire window with minimal UV absorption is used as the OES port. The emission spectra are taken 1 in. above the substrate surface in this study so that gas phase information near the wafer surface can be collected.

Table 1. OES channel configurations of wavelength range, start pixel (SP), end pixel (EP) and resolution (in full width at half maximum [FWHM]).

CH	Range (nm)	SP	EP	Res.[FWHM]
0	196.14 ∼ 354.44	4	2044	1.5
1	327.23 ∼ 464.27	0	2047	1.4
2	437.93 ∼ 617.89	0	2047	1.8
3	585.70 ∼ 868.81	0	2046	2.8
4	786.50 ∼ 1039.51	1	2047	2.5

Table 2. Transitions and wavelengths of atomic emissions observed.

(Striganov and Sventitskii, 1968)

Species	Wavelength (nm)	Transition
Ar	750.39	$4s'_{(1/2)}{}^{o} - 4p'_{(1/2)}$
C	247.85	$2p^2\,{}^1S - 3s^1\,4P^o$
H_β	486.13	$2p^2P^o - 4d^2D$
O	777.42	$3s^5S^o - 3p^5P$
Zr	350.93	
	351.96	
Zr^+	339.20	N/A
	343.82	
	349.62	

The major atomic emission peaks and molecular band heads observed in this study are summarized in Table 2 and Table 3, respectively. The analog signals produced by optical channels are captured by an Ocean Optics ADC1000 high-speed ISA-bus A/D converter installed in a Pentium PC. The OES data are then transmitted through fast ethernet to the computer used for real-time process control.

Table 3. Transitions and wavelengths of molecular emissions observed.

(Pearse and Gaydon, 1976)

Species	Wavelength (nm)	Transition
C_2	516.52	$A^3\Pi_g - X^3\Pi_u$
CH	431.42	$A^2\Delta - X^2\Pi$

4. FEEDBACK CONTROL SYSTEM: DESIGN AND IMPLEMENTATION

The carbon content of the thin film can not be measured directly in real-time, and thus, estimates of the carbon content, which are obtained based on plasma composition in the reactor chamber by OES, are used in the feedback control system. Previous spectroscopic study of the reaction plasma (Cho *et al.*, 2001) in this ECR PECVD system has shown that the carbon content in the film has a quasi-linear relationship with respect to the optical emission intensity ratio of C_2 molecules and O atoms in the reacting gas. This can be explained by the fact that carbon molecules are mostly responsible in forming the precursors for carbon incorporation into the film. This result suggests that the information of optical emission intensity ratio of C_2/O can be utilized to estimate the carbon content in the zirconium dioxide film in real-time.

In this work, a mathematical model is constructed to estimate the carbon content of the film based on the optical emission intensity ratio which is obtained through OES in real-time. Following the previous experimental results (Cho *et al.*, 2001), the relationship between the carbon content in the surface layer and the optical emission intensity ratio can be written as follows:

$$X_C^s(t) = A\gamma(t) \tag{1}$$

where X_C^s is the atomic concentration (%) of carbon in the surface of the film, A is a constant which is related to the operating condition of the specific experimental system (experimentally determined for our current chamber condition to be 11.92) and γ is the optical emission intensity ratio of C_2/O.

Under the assumption that the film growth rate remains constant, the carbon content of the whole film is obtained using the following formula:

$$X_C(t) = \frac{\int_{t_0}^{t} X_C^s(s)ds}{t - t_0} \tag{2}$$

where X_C is the atomic concentration (%) of carbon in the bulk of the deposited film at time t and t_0 is the time in which the deposition starts. In this case, we treat X_C as the time average of X_C^s. Combining Eqs. 1 and 2, the following estimation model is obtained:

$$X_C(t) = A\frac{\int_{t_0}^{t} \gamma(s)ds}{t - t_0} \tag{3}$$

We note that although the deposition process is a batch process in nature, an optimal operating recipe can not be obtained since no accurate mathematical model describing the relationship between the optical emission intensity ratio and the inlet mass flow rate is currently available. Thus, the control problem for the process is formulated as a set-point regulation problem; this approach is further justified by our experimental results which clearly show that the response time of the closed-loop system is significantly smaller than the total deposition time.

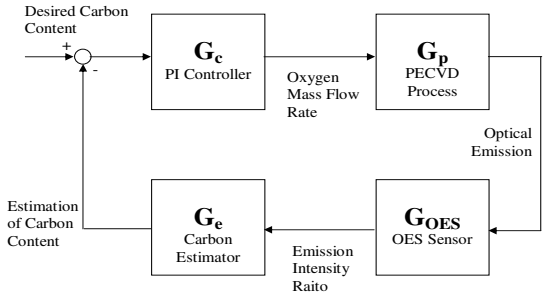

Fig. 3. Block diagram of the closed-loop system under the proposed carbon content controller.

Figure 3 shows the structure of the closed-loop system under the proposed carbon content controller. The input to the controller is the difference between the desired carbon content and the estimated carbon content and the controller manipulates the inlet oxygen mass flow rate. The sensor block G_{OES} can be treated as a pure time delay since it takes a fixed amount of integration time for the OES system to obtain good signal-to-noise ratios and transfer the OES data through the network. The G_e block is the carbon estimator described above. The G_c block is the controller based on the proportional-integral (PI) control algorithm (described below in detail). The G_p block is the process block describing the relationship between the change of oxygen mass flow rate and the optical emission intensity ratio γ of the plasma. G_p is identified experimentally and the identification procedure will be discussed in detail in subsection 5.1 below.

To eliminate unnecessary control actions, which may interfere with the plasma and lead to poor closed-loop performance, the control objective is to stabilize the carbon content value close to the desired set-point (i.e., within a certain tolerance ε). A PI control algorithm is used to achieve this objective of the following form:

$$\frac{f_{Ar}(t)}{f_{O_2}(t)} = U(t) = K_c\hat{e}(t) + K_i\int_{t_0}^{t}\hat{e}(\mu)d\mu + \bar{R}_f \quad (4)$$

$$\hat{e}(t) = \begin{cases} e(t) & |e(t)| > \varepsilon \\ 0 & |e(t)| \le \varepsilon \end{cases} \quad (5)$$

where U is the output of the controller (i.e., the mass flow ratio of Ar/O_2), $\bar{R}_f$ is a steady state bias expressed in terms of the mass flow ratio of Ar/O_2 at steady state, f_{O_2} is the oxygen mass flow rate, f_{Ar} is the Argon mass flow rate which scales with the precursor vapor flow rate, e is the difference between the estimated carbon content and the set-point value, K_c is the proportional gain and K_i is the integral gain. The input of the controller $\hat{e}(t)$ is defined as in Eq.5 where ε is the tolerance within which we want to approach the desired set-point.

MATLAB simulations of the entire process model were performed to obtain reference values of the controller parameters to be used in the real-time computer control system. The reference values were initially computed by using the Ziegler Nichols (ZN) tuning method (e.g. (Coughanowr, 1991)) and then adjusted based on simulation results to achieve a desired closed-loop response.

The computer process control system was implemented on an Intel Pentium III 700 MHz PC with 512 MByte RAM. All the programs used in this study were written in LabVIEW language and National Instruments LabVIEW for Windows Version 6.1 was used as runtime platform.

5. EXPERIMENTAL RESULTS AND DISCUSSION

5.1 *Open-loop system*

The objective of the open-loop experiments is to study the dynamic behavior of the deposition process based on real-time OES measurements.

The first set of experiments (3 independent runs) were performed to study the relationship between the steady-state value of γ and the mass flow ratio of Ar/O_2, R_f. The experimental results are shown in Figure 4; each data point is obtained by setting R_f at a fixed value and measuring γ after 200 s to guarantee that the process has reached steady-state. The experimental results in Figure 4 suggest that the optical emission intensity ratio varies proportionally with respect to the cubic of the mass flow rate ratio; this relationship is shown by the dotted line and can be mathematically expressed as follows:

$$\gamma_{ss} = K_p R_f^3 \quad (6)$$

where γ_{ss} is the steady-state value of the optical emission intensity ratio and K_p is a constant which depends on the processing chamber conditions and the carrier gas flow rate.

In the second experiment, the process dynamics are identified by varying the mass flow ratio R_f in a way shown in the top curve in Figure 5 and measuring γ in real time using OES; the experimental results are presented in Figure 5. It can been seen that the process can be approximated by a first-order system which has a small time constant.

Using the experimental results shown in Figures 4 and 5, we constructed a *Simulink* model shown in

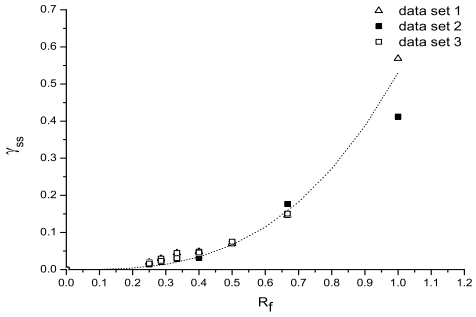

Fig. 4. Experimental data of R_f vs. γ_{ss} from different depositions for fixed argon flow rate 8 sccm, chamber pressure at 40 mTorr and microwave power 300 W.

Figure 6 within a MATLAB environment to simulate the process; $R_f(t)$ is the input and $\gamma(t)$ is the output. The model parameters were identified from the experiments to be K_p=0.53 and τ_p=10 s.

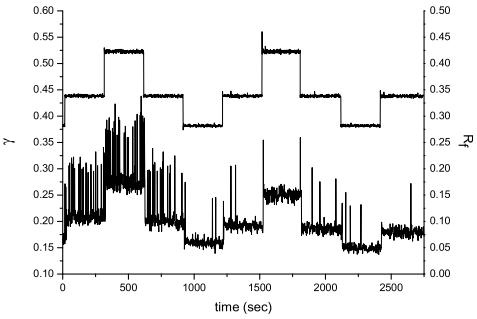

Fig. 5. Response curve of γ for step changes in R_f for argon flow rate 8 sccm, chamber pressure 40 mTorr and microwave power 300 W.

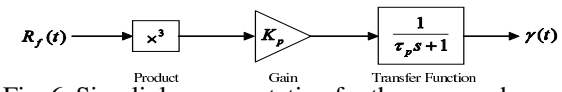

Fig. 6. Simulink representation for the process dynamics.

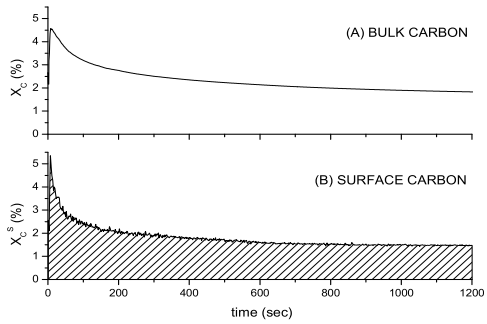

Fig. 7. Profiles of bulk (A) and surface (B) carbon concentration of a ZrO_2 film computed based on real-time OES measurements during an open-loop deposition with microwave power 300 W, chamber pressure 40 mTorr, Ar flow rate 8.4 sccm and O_2 flow rate 8 sccm.

Figure 7 shows the evolutions of the carbon concentration of the surface (A) and of the bulk (B) of a ZrO_2 film during a typical open-loop deposition. The carbon concentrations are computed based on real-time OES measurements using the proposed estimation model. It can be observed that the starting stage of the deposition has relatively higher carbon incorporation. This corresponds to the OES measured high C_2 emission intensity and low O emission intensity during the initial stage of the deposition, as shown in Figure 8. Low O emission intensity indicates a low O concentration in the plasma; this may cause incomplete oxidation of the precursor, which leads to a high concentration of C_2 in the plasma during the initiation of the deposition process.

It can also be noticed in Figure 7 that the carbon concentration of the bulk of the film changes throughout the deposition process. This is not only because the bulk carbon concentration is an average value, but also because the carbon incorporation rate varies with time. This time variation may be explained by the continuous increase of O concentration in the plasma due to the complex and competing serial oxidation and dissociation processes (Cho *et al.*, 2002). As a result, reaction products with different compositions are generated and different amount of carbon is incorporated into the film at different times during the deposition process. Due to the existence of these uncertainties in the deposition process, the profile of bulk concentration of carbon shown in Figure 7 is not reproducible in our experiments; this suggests that it is very difficult to obtain a desired carbon concentration with open-loop operation.

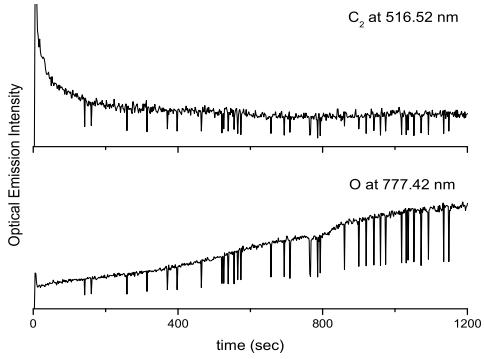

Fig. 8. Profiles of C_2 and O optical emission intensity during an open-loop deposition with microwave power 300 W, chamber pressure 40 mTorr, Ar flow rate 8.4 sccm and O_2 flow rate 8 sccm.

5.2 *Evolution of the closed-loop system*

Using the developed real-time feedback control system, a carbon content-controlled deposition experiment was performed (see (Ni *et al.*, 2003) for more results of closed-loop deposition experiments). Figure 9 shows a 20-minute long controlled-deposition which was carried out with microwave power fixed at 300 W, chamber pressure controlled at 40 mTorr and Ar flow rate set at 8 sccm. The carbon content controller was implemented with a set-point value for the atomic car-

bon concentration of 1.4%, proportional gain K_c=1.0, integral gain K_I=0.05 and error tolerance ε=0.03%.

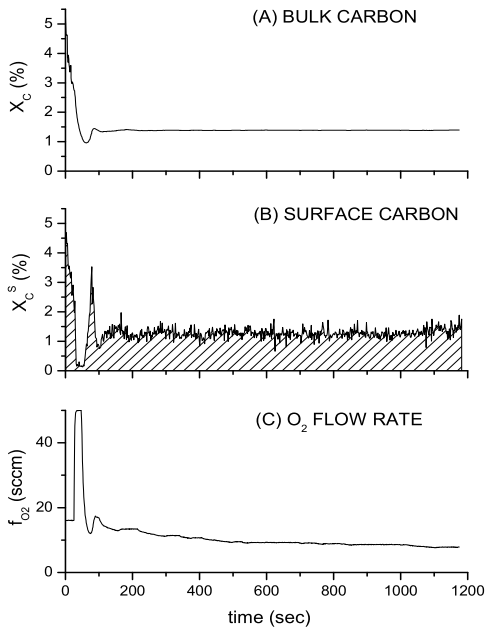

Fig. 9. Profiles of bulk (A) and surface (B) carbon concentration of a ZrO_2 film computed based on real-time OES measurements and profile of manipulated oxygen flow rate (C) during a controlled deposition experiment with microwave power 300 W, chamber pressure 40 mTorr and Ar flow rate 8.4 sccm.

From the bulk carbon concentration curve in Figure 9, we can see that the carbon content of the film was controlled very closely to the desired value of 1.4% in spite of the initial plasma disturbance mentioned above (this result was also verified through off-line XPS analysis of the deposited film; see (Ni *et al.*, 2003) for details). The response time is relatively small compared to the deposition duration which supports our set-point regulation formulation of this control problem.

Comparing the bulk carbon concentration profile of the thin films under closed-loop (Figure 9, top plot) and open-loop (Figure 7, top plot) conditions with the same initial deposition conditions, it can be clearly seen that the carbon content of the film was reduced by more than a factor of 5 under closed-loop control. Moreover, compared to open-loop operation, the controlled process is more robust with respect to disturbances caused by system start-up, and mass flow rate and plasma variations.

6. REFERENCES

Armaou, A. and P. D. Christofides (1999). Plasma-enhanced chemical vapor deposition: Modeling and control. *Chem. Eng. Sci.* **54**, 3305–3314.

Armaou, A., J. Baker and P. D. Christofides (2001). Feedback control of plasma etching reactors for improved etching uniformity. *Chem. Eng. Sci.* **56**, 1467–1475.

Chaneliere, C., J. L. Autran, R. A. B. Devine and B. Balland (1998). Tantalum pentoxide (Ta_2O_5) thin films for advanced dielectric applications. *Mater. Sci. Eng., R.* **22**, 269–322.

Cho, B. O., J. Wang and J. P. Chang (2002). Metalorganic precursor decomposition and oxidation mechanisms in plasma-enhanced ZrO_2 deposition. *J. Appl. Phys.* **92**(8), 4238.

Cho, B. O., S. Lao, L. Sha and J. P. Chang (2001). Spectroscopic study of plasma using zirconium tetra-tert-butoxide for the plasma enhanced chemical vapor deposition of zirconium oxide. *J. Vac. Sci. Tech. A* **19**(6), 2751.

Copel, M., M. Gribelyuk and E.P. Gusev (2000). Structure and stability of ultrathin zirconium oxide layers on Si(001). *Appl. Phys. Lett.* **76**, 436–438.

Coughanowr, D. R. (1991). *Process Systems Analysis and Control*. McGraw-Hill. New York.

Frenck, H. J., E. Oesterschulze, R. Beckmann, W. Kulisch and R. Kassing (1991). Low temperature remote plasma-enhanced deposition of thin metal oxide films by decomposition of metal alkoxides. *Mater. Sci. Eng.A* **139**, 394–400.

Iwai, H. and H. S. Momose (1998). Ultra-thin gate oxides performance and reliability. *IEDM Tech. Dig.* pp. 163–166.

Lo, S. H., D. A. Buchanan, Y. Taur and W. Wang (1997). Quantum-mechanical modeling of electron tunneling current from the inversion layer of ultra-thin-oxide nMOSFET's. *IEEE Electron. Device Lett.* **18**, 209–211.

Maury, F., L. Gueroudji and C. Vahlas (1996). Selection of metalorganic precursors for MOCVD of metallurgical coatings: Application to Cr-based coatings. *Surf. Coat. Technol.* **87**, 316–324.

Ni, D., Y. Lou, P. D. Christofides, L. Sha, S. Lao and J. P. Chang (2003). A method for real-time control of thin film composition using OES and XPS. In: *Proceedings of the American Control Conference*. Denver, Colorado.

Pearse, R. W. B. and A. G. Gaydon (1976). *The Identification of Molecular Spectra*. Wiley. New York.

Striganov, A. R. and N. S. Sventitskii (1968). *Tables of Spectral Lines of Neutral and Ionized Atoms*. IFI/Plenum. New York.

Vahlas, C., F. Maury and L. Gueroudji (1998). A thermodynamic approach to the CVD of chromium and of chromium carbides starting from Cr(C_6H_6)(2). *Chem. Vap. Deposition* **4**, 69–76.